

but arrested with an elongated bud, lacking a bipolar mitotic spindle (Fig. 5). This phenotype is consistent with our findings that overexpression of *CDH1* induces degradation of mitotic cyclins.

We have identified a family of highly conserved WD40-repeat proteins as limiting activators of APC-dependent proteolysis. Cdc20 and Cdh1 were not general activators of APC-dependent proteolysis, but instead they appeared to be substrate specific. The WD40-repeat protein Cdc4 also serves as a specificity factor in the degradation of substrates of the Skp1/Cdc53-dependent proteolysis machinery (27). Specificity factors may facilitate the differential regulation of various substrates ubiquitinated by the same ubiquitination machinery. Cdc20 and Cdh1 may ensure that different substrates of the APC are degraded at the right time during M phase. Cdc20 may target APC substrates whose degradation is required for the metaphase-anaphase transition (such as Pds1) for degradation, whereas Cdh1 may trigger destruction of substrates whose degradation is important for exit from M phase (such as Clb2 and Ase1). Cdc20 homologs in other species may also be substrate-specific activators of APC-dependent proteolysis.

REFERENCES AND NOTES

1. O. Cohen-Fix, J.-M. Peters, M. W. Kirschner, D. Koshland, *Genes Dev.* **10**, 3081 (1996).
2. R. W. King, R. J. Deshaies, J.-M. Peters, M. W. Kirschner, *Science* **274**, 1652 (1996).
3. Y.-L. Juang *et al.*, *ibid.* **275**, 1311 (1997).
4. R. W. King *et al.*, *Cell* **81**, 279 (1995).
5. V. Sudakin *et al.*, *Mol. Biol. Cell* **6**, 185 (1995).
6. T. Evans, E. T. Rosenthal, J. Youngblom, D. Distel, T. Hunt, *Cell* **33**, 389 (1983).
7. A. Amon, S. Irmiger, K. Nasmyth, *ibid.* **77**, 1037 (1994).
8. M. Brandeis and T. Hunt, *EMBO J.* **15**, 5280 (1996).
9. W. G. Whitfield, C. Gonzalez, G. Maldonado-Codina, D. M. Glover, *ibid.* **9**, 2563 (1990).
10. T. Hunt, F. C. Luca, J. V. Ruderman, *J. Cell Biol.* **116**, 707 (1992).
11. S. Sigrist, H. Jakobs, R. Stratmann, C. F. Lehner, *EMBO J.* **14**, 4827 (1995).
12. N. Sethi, M. C. Monteagudo, D. Koshland, E. Hogan, D. J. Burke, *Mol. Cell. Biol.* **11**, 5592 (1991).
13. I. A. Dawson, S. Roth, S. Artavanis-Tsakonas, *Development* **117**, 359 (1993).
14. ———, *ibid.* **129**, 725 (1995).
15. W. Zachariae and K. Nasmyth, *Mol. Biol. Cell* **7**, 791 (1996).
16. All strains were derivatives of strain W303. *CLB2*, *PDS1*, and *ASE1* constructs were as described (1, 3, 7). Immunoprecipitations of <sup>35</sup>S-labeled Clb2 protein and DNA content analysis were performed as described (7). Protein immunoblot analysis of the total amount of Pds1, Ase1, and Cdc28 was done as described (1, 7).
17. To generate a *GAL-CDC20* fusion, we engineered a Bgl II site at the AUG of *CDC20* and ligated it to an Eco RI to Bam HI fragment carrying the *GAL1-10* promoter. The fusion was integrated at the *URA3* locus.
18. R. Visintin, S. Prinz, A. Amon, unpublished observations.
19. W. R. Pearson and D. J. Lipman, *Proc. Natl. Acad. Sci. U.S.A.* **85**, 2444 (1988).
20. The probability score for Cdc20 and YGL003Cp being randomly related was  $8 \times 10^{-30}$ . The next lowest score was  $3 \times 10^{-6}$  for the ORF YRC72C, which also encodes a putative WD40-repeat protein.

21. S. F. Altschul, W. Gish, W. Miller, E. W. Myers, D. J. Lipman, *J. Mol. Biol.* **251**, 403 (1990).
22. A 1.8-kb fragment containing the *CDH1* gene was isolated from total genomic DNA by polymerase chain reaction. The *HIS3* gene was used to replace the *CDH1* ORF between the Nhe I and Bln I sites. The 1.8-kb fragment containing the *CDH1* gene was also used to generate a *GAL-CDH1* fusion that was integrated at the *URA3* locus.
23. Small G<sub>1</sub> phase daughter cells were elutriated as described (28). Nocodazole and hydroxyurea were added at concentrations of 15 μg/ml and 10 mg/ml, respectively.
24. M. D. Mendenhall, *Science* **259**, 216 (1993).
25. A. Amon, M. Tyers, B. Futcher, K. Nasmyth, *Cell* **74**, 993 (1993).
26. I. Fitch *et al.*, *Mol. Biol. Cell* **3**, 805 (1992).
27. D. Skowrya *et al.*, *Cell*, in press.
28. E. Schwob and K. Nasmyth, *Genes Dev.* **7**, 1160 (1993).
29. S. Irmiger, S. Piatti, M. Michaelis, K. Nasmyth, *Cell* **87**, 269 (1995).
30. We thank O. Cohen-Fix, D. Koshland, and D. Pellman for antibodies and plasmids and V. Siegel, O. Cohen-Fix, D. Koshland, D. Pellman, S. Bell, D. Pellman, H. Madhani, T. Orr-Weaver, V. Mayer, A. Page, and M. Lane for helpful discussions and critical reading of the manuscript.

24 July 1997; accepted 19 September 1997

## Forward and Backward Propagation of Dendritic Impulses and Their Synaptic Control in Mitral Cells

Wei R. Chen,\* Jens Midtgaard, Gordon M. Shepherd

The site of impulse initiation is crucial for the integrative actions of mammalian central neurons, but this question is currently controversial. Some recent studies support classical evidence that the impulse always arises in the soma-axon hillock region, with back-propagation through excitable dendrites, whereas others indicate that the dendrites are sufficiently excitable to initiate impulses that propagate forward along the dendrite to the soma-axon hillock. This issue has been addressed in the olfactory mitral cell, in which excitatory synaptic input is restricted to the distal tuft of a single primary dendrite. In rat olfactory bulb slices, dual whole cell recordings were made at or near the soma and from distal sites on the primary dendrite. The results show that the impulse can be initiated in either the soma-axon hillock or in the distal primary dendrite, and that the initiation site is controlled physiologically by the excitatory synaptic inputs to the distal tuft and inhibitory synaptic inputs near the soma.

The mitral cell of the mammalian olfactory bulb gives rise to one apical dendrite (termed primary dendrite) and several lateral basal dendrites (termed secondary dendrites) (1). The primary dendrite extends 200 to 350 μm in the rat and enters a single glomerulus, where it ramifies in a distal tuft of branches that receive excitatory synaptic input from terminals of olfactory nerve (ON) (Fig. 1A). The secondary dendrites extend horizontally in the external plexiform layer (EPL), mediating recurrent and lateral synaptic inhibition through reciprocal dendrodendritic synapses with inhibitory granule cell interneurons (2).

As inferred by Ramon y Cajal in 1911 and established by later authors (1), the main function of the primary dendrite is clear: It links the synaptic response to olfactory input in the distal tuft to impulse output in the axon. This has served as one

of the best examples proving that distal dendritic input is not limited to slow background modulation of soma output, but can mediate rapid information transmission (3). The location of excitatory synapses exclusively on the distal tuft thus furnishes an attractive model for investigating the role of dendrites in linking excitatory synaptic input to impulse output in a mammalian central neuron. In addition, the entirely separate location of granule cell inhibitory input to the soma and secondary dendrites provides a model for investigating the control of excitatory dendritic responses by synaptic inhibition.

Mitral cells were visualized in thick tissue slices of rat olfactory bulb under an infrared differential interference contrast (DIC) microscope (4–6). Primary dendrites were clearly visible and could be traced from the cell bodies all the way into individual glomeruli. Simultaneous whole cell recordings were made from the soma and at various distal sites on the primary dendrite near the glomerular tuft (n = 24 pairs from 22 slices). Dual dendritic recordings from proximal and distal sites (Fig. 1B; n = 5) gave results similar to those from soma and

W. R. Chen and G. M. Shepherd, Section of Neurobiology, Yale University School of Medicine, New Haven, CT 06510, USA.

J. Midtgaard, Department of Medical Physiology, University of Copenhagen, DK-2200 N, Copenhagen, Denmark.

\*To whom correspondence should be addressed.

distal sites. In all recordings, fast action potentials were observed in both soma and distal dendrite.

Excitatory postsynaptic potentials (EPSPs) were evoked in mitral cells by stimulation of the olfactory nerve layer. A single shock to the ON evoked an EPSP that was always larger at the distal dendritic recording site, consistent with the synaptic input being confined to the distal glomerular tuft (Fig. 1, B and C;  $n = 17$ ). When the ON stimuli were weak, the action potentials arising from this EPSP occurred first at or near the soma and second at the distal dendritic recording site (Fig. 1B; two impulse pairs on the right;  $n = 17$ ). This finding is consistent with axosomatic initiation followed by back-propagation of impulses, as observed in neocortical and hippocampal pyramidal cells (7). However, as the stimulus intensity increased, action-potential initiation shifted to the distal primary dendrite, followed by an action potential at the near-soma site (Fig. 1B, leftmost impulse pair;  $n = 14$ ). Both the somatic and dendritic impulses, when evoked by current pulse injection, were blocked by  $1 \mu\text{M}$  tetrodotoxin in the bath, indicating that these fast action potentials were dependent on the activation of sodium channels [(8);  $n = 5$ ]. The higher levels of synaptic excitation presumably correspond to stronger odor stimulation, which in vivo elicits large-amplitude slow potentials across the glomeruli, and large amplitude EPSPs giving rise to burst re-

sponses in mitral cells (9).

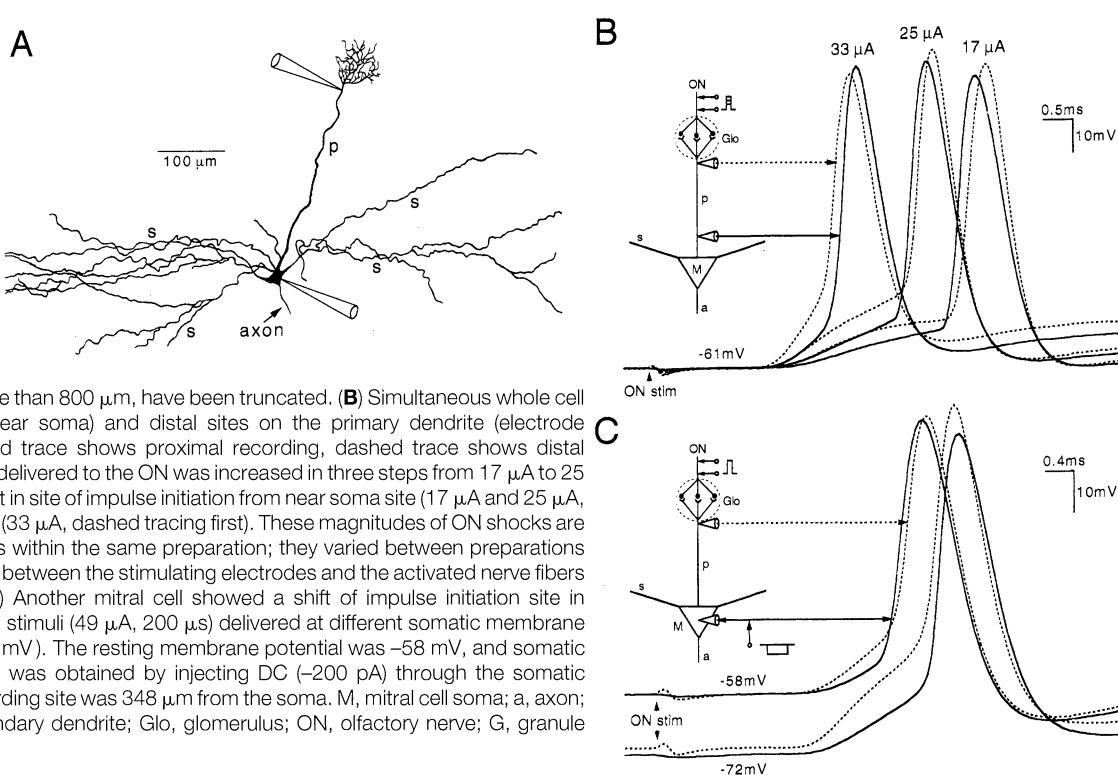
To rule out possible effects of whole cell patch break-in, dual recordings of small amplitude extracellular spikes were made before break-in [(8);  $n = 8$ ]. These spikes showed the same shift in initiation site with increasing ON synaptic input. After patch break-in, the mitral cells had resting potentials of  $-55$  to  $-65$  mV, and some cells spontaneously fired action potentials, similar to properties seen in vivo (9). Possible initiation of impulses from an axon of dendritic origin [as in substantia nigra neurons (10)] was ruled out by staining the dually recorded mitral cells with fluorescent dyes and biocytin ( $n = 8$ ); in all cases, the axon was found to emerge from the cell body (Fig. 1A), as described previously in a number of morphological studies (1).

In addition to being dependent on excitatory synaptic input, the impulse initiation site was also dependent on inhibitory input. With weak ON stimuli, the somatically initiated impulse could be blocked by hyperpolarizing the somatic membrane, or by an inhibitory postsynaptic potential (IPSP) elicited by a single shock to the EPL (8). With moderate ON stimuli, however, the site of impulse initiation could be shifted from soma to distal dendrite by soma hyperpolarizing current injection (Fig. 1C;  $n = 10$ ). The same result could be obtained by an EPL-evoked IPSP. This IPSP was always larger at the soma than at the distal primary dendrite (Fig. 2, A and C;  $n = 9$ ), consis-

tent with passive spread of the IPSP into the distal primary dendrite from dendrodendritic synapses located at the secondary dendrites and soma (1–3). The IPSP could change the initiation site and propagation direction of an impulse evoked either by distal primary dendrite current injection (Fig. 2, A and B;  $n = 3$ ) or by ON excitatory synaptic input (Fig. 2, C and D;  $n = 5$ ). Thus, it appeared that both the excitatory synaptic input at the distal primary dendrite and the granule cell inhibition close to the soma can control the relative excitability between soma and distal primary dendrite and thereby change the site of impulse initiation and direction of impulse propagation. Even when impulse initiation would normally occur at the soma, a distal dendritic hot spot can provide a means for a nerve cell to overcome inhibition at the soma.

A classic sign of distal dendritic excitability is a fast prepotential recorded from the soma, as first shown in hippocampal pyramidal cells (11). This type of response has been seen in intracellular studies (6, 12) in vitro in the turtle and rat olfactory bulb, as well as in vivo in the rabbit. A fast prepotential was sometimes observed in our paired recordings ( $n = 7$ ) (Fig. 3, A and B). In the first of two consecutive sweeps (trace 1 in Fig. 3A), the full-size somatic impulse, which lagged the corresponding dendritic impulse, was preceded by a small prepotential (single arrow) that also occurred later

**Fig. 1.** Increasing dendritic synaptic excitation or hyperpolarizing somatic membrane potential shifted action-potential initiation from near the soma to the distal primary dendrite. **(A)** Morphology of a biocytin-stained mitral cell simultaneously recorded from the soma and the distal primary dendrite as indicated. Note that the axon originated from the base of the cell body. Some secondary dendrites, which extended horizontally for more than  $800 \mu\text{m}$ , have been truncated. **(B)** Simultaneous whole cell recordings from proximal (near soma) and distal sites on the primary dendrite (electrode distance:  $217 \mu\text{m}$ ). The solid trace shows proximal recording, dashed trace shows distal recording. Stimulus strength delivered to the ON was increased in three steps from  $17 \mu\text{A}$  to  $25 \mu\text{A}$  to  $33 \mu\text{A}$ , producing a shift in site of impulse initiation from near soma site ( $17 \mu\text{A}$  and  $25 \mu\text{A}$ , solid tracing first) to distal site ( $33 \mu\text{A}$ , dashed tracing first). These magnitudes of ON shocks are relevant only for comparisons within the same preparation; they varied between preparations because of varying distances between the stimulating electrodes and the activated nerve fibers (see also Figs. 2 and 3). **(C)** Another mitral cell showed a shift of impulse initiation site in response to two identical ON stimuli ( $49 \mu\text{A}$ ,  $200 \mu\text{s}$ ) delivered at different somatic membrane potential levels ( $-58$  and  $-72$  mV). The resting membrane potential was  $-58$  mV, and somatic membrane hyperpolarization was obtained by injecting DC ( $-200$  pA) through the somatic electrode. The dendritic recording site was  $348 \mu\text{m}$  from the soma. M, mitral cell soma; a, axon; p, primary dendrite; s, secondary dendrite; Glo, glomerulus; ON, olfactory nerve; G, granule cell.



than the dendritic impulse (see Fig. 3B, top, for comparison of the somatic and dendritic impulses). In the second sweep (trace 2 in Fig. 3A), in which the soma was slightly hyperpolarized, the full-size somatic impulse failed, yielding an isolated prepotential (double arrow) that appeared to be caused by passive spread of the dendritic impulse to the soma (see Fig. 3B, bottom, for comparison with the dendritic impulse). Occasionally, an EPL-evoked IPSP was strong enough to block forward propagation (Fig. 3, C and D;  $n = 4$ ), leaving at the soma a small prepotential (trace 4, single arrow) reminiscent of a dendritic action potential (trace 2). This indicates that an action potential can be initiated independently in the distal dendrite, even without pairing with a somatic action potential.

These results provide a perspective on current questions concerning the site of impulse initiation in mammalian central neurons. It is well known that dendrites in many types of neurons generate  $\text{Na}^+$  impulses (13). In hippocampal and neocortical pyramidal cells, for example, weak excitatory synaptic activation at impulse threshold elicits a somatic impulse which back-propagates into the dendrites (7). There has been evidence that at higher excitation intensities, the impulse trigger zone can shift to the apical dendrites (14). However, it has been suggested that this orthodromically elicited dendritic impulse is a purely local event occurring only during very strong excitation, that any excitable response of the dendrites is not able to propagate effectively to the soma and axon and therefore should be considered an active form of synaptic integration rather than action-potential initiation, and that the axon initial segment is the only site for impulse initiation at all intensities of synaptic input in mammalian central neurons (15).

Our recordings confirm that the classical model applies to the mitral cell at weak levels of synaptic excitation, when the impulse is initiated at the axosomatic region and back-propagates into the dendrites. Both somatic and dendritic impulses are  $\text{Na}^+$ -dependent. With increasing intensity of dendritic depolarization, active responses of the dendrites are initiated, as has also been reported in other neurons (7, 14, 15). Our findings are that in the mitral cell, this distal dendritic activity consists of an impulse that has a large amplitude and rapid time course; it leads directly to impulse generation at the soma, and this link appears to be quite reliable.

The results further show that in a range of EPSP amplitude where the classical model of somatic impulse initiation applies, proximal inhibitory input can shift the im-

pulse origin for the same EPSP to the distal dendrite and change the direction of impulse propagation in the dendrite from backward to forward. These mechanisms likely play critical roles in sensory responses under physiological conditions. It may be postulated that both the large-amplitude EPSPs and large-amplitude IPSPs recorded in vivo in response to strong odor stimulation [(9); see above] function in a coordinated manner to shift impulse initiation to the distal dendrites. This could ensure that the distal tuft continues to respond actively to excitatory input despite the shutdown of impulse output in the axon. Further in vivo studies are needed to test directly for these mechanisms.

How broadly might these properties of mitral cells generalize to other neurons? Although the distal dendritic tuft is specialized for specific sensory input, this arrangement has similarities with pyramidal cells, where the lamination of inputs provides for

discrete synaptic sites, both for excitation to the distal apical tuft and inhibition to the axon hillock (16). Distal (layer I) synaptic stimulation in neocortical pyramidal cells can evoke an axosomatic back-propagating impulse (7), as is the case in mitral cells with weak to moderate dendritic excitation. Computer simulations (17) have supported the experimental evidence (13, 14) that forward-propagating fast sodium action potentials can be initiated in the apical dendrites of mature cortical pyramidal neurons. With regard to synaptic influences on impulse propagation in dendrites, it is known that synaptic inhibition can control the extent of dendritic invasion of a back-propagating impulse in cerebellar Purkinje cells and hippocampal pyramidal neurons (18). Further studies are needed to determine whether proximal inhibition in Purkinje cells by basket cells and in pyramidal neurons by chandelier cells could, in addition, shift

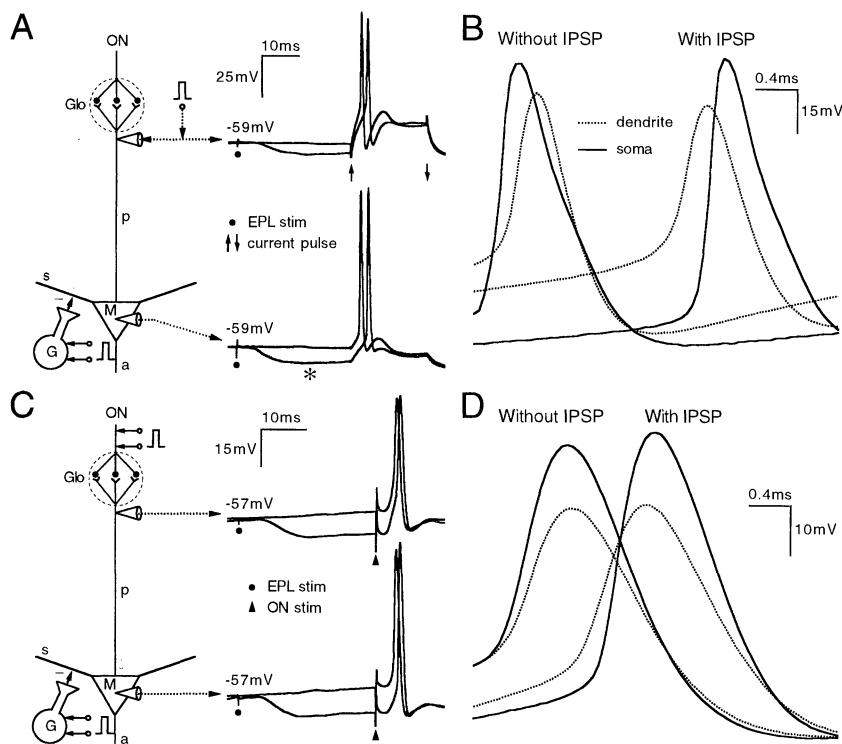


**Fig. 2.** Inhibitory synaptic input near the soma shifted action-potential initiation from soma to distal dendrite. **(A)** Effect of an IPSP on impulse initiation evoked by a brief depolarizing current pulse (120 pA, 20 ms) injected into the distal primary dendrite. Upper panel: dendritic recording. Lower panel: somatic recording. Two traces are superimposed in each panel: control response to the current pulse and test response preceded by a shock (20  $\mu\text{A}$ , 200  $\mu\text{s}$ ) delivered laterally in the deep EPL to evoke a slow, long-latency IPSP in the secondary dendrites of the recorded cell [accordingly, the IPSP was larger at the soma (\*) than at the dendritic recording site]. The dendritic recording site was 314  $\mu\text{m}$  from the soma. **(B)** An expanded view of the evoked action potentials in (A), to show the shift in impulse initiation site. **(C)** Effect of an IPSP on impulse initiation evoked in another mitral cell by synaptic excitation of the distal dendrite. ON shocks (100  $\mu\text{A}$ , 200  $\mu\text{s}$ ) were delivered (see arrowheads) to evoke an EPSP-generated action potential in the absence and presence of an IPSP from a preceding EPL shock (filled circle: 200  $\mu\text{A}$ , 200  $\mu\text{s}$ ). The dendritic recording site was 305  $\mu\text{m}$  from the soma. **(D)** An expanded view of the ON-evoked action potentials in (C), showing the shift in impulse initiation from slightly earlier in the soma (without IPSP) to earlier in the dendrite (with IPSP). For diagram abbreviations, see Fig. 1 caption.

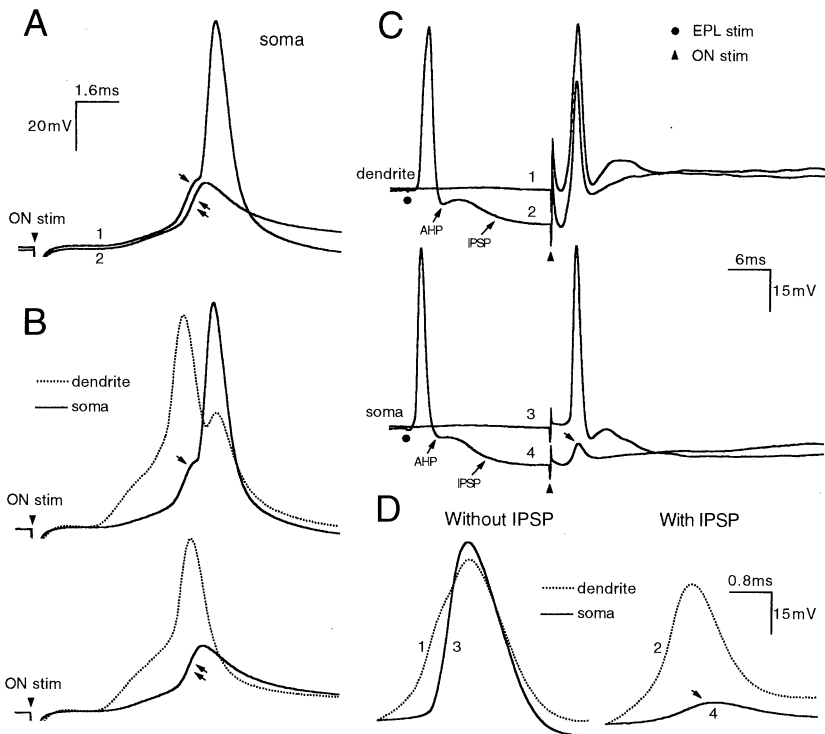


**Fig. 3.** Fast prepotentials recorded at the mitral cell soma were always correlated with a dendritic action potential. **(A)** Threshold ON stimulation (400  $\mu$ A, 200  $\mu$ s) evoked in the mitral cell soma a full-size action potential that was preceded by a small prepotential (single arrow, trace 1). Occasionally, the same stimulation failed to evoke a full-size action potential, yielding an isolated fast prepotential (double arrow, trace 2) at the soma. Membrane potential (with  $-290$  pA DC injection) was  $-80$  mV. **(B)** Comparisons of dendritic recordings (dashed line) with their corresponding somatic recordings (solid line) shown in traces 1 and 2 of **(A)**, respectively, for the case when the prepotential elicited a soma impulse (top) and when it failed (bottom). The dendritic recording site was  $223$   $\mu$ m from the soma. **(C)** Inhibitory synaptic input near the soma blocked forward propagation of a dendritic impulse, yielding a small somatic prepotential (single arrow, trace 4). Traces 1 and 2 are dendritic recordings, whereas traces 3 and 4 are simultaneous somatic recordings. Traces 1 and 3 are control ON stimulation without prior EPL stimulation; traces 2 and 4 are the EPL-ON sequential activation. EPL stimulation evoked an IPSP that was preceded by an action potential, which was due to direct stimulation of the secondary dendrites of the recorded cell. The IPSP was differentiated from the spike afterhyperpolarization (AHP) by its blockade with  $30$   $\mu$ M bicuculline methiodide (8). EPL stimulation:  $20$   $\mu$ A,  $200$   $\mu$ s. ON stimulation:  $100$   $\mu$ A,  $200$   $\mu$ s. The dendritic recording site was  $286$   $\mu$ m from the soma. **(D)** An expanded view of the ON-evoked action potentials in **(C)**. Left panel, control traces 1 and 3 without IPSP; right panel, traces 2 and 4 with preceding IPSP.

impulse origin to the dendrites. In these types of neurons that are under strong inhibition at or near the axon hillock, distal dendritic electrogenesis such as we describe in mitral cells provides a means of overcoming that inhibition and thus extending the operating range of the cell. Furthermore, even when impulse output from the axon hillock is inhibited, the dendritic impulse can continue to evoke local  $Ca^{2+}$  influx (18) that enables the distal dendrites to continue to be involved in local processes, such as dendritic release of transmitters or synaptic plasticity.

In summary, mitral cells provide a model for multiple impulse initiation sites within a neuron that explains how they may be controlled by both excitatory and inhibitory synaptic inputs. This model helps to widen

the view of how dendritic excitability contributes to processing of information in different types of neurons in the vertebrate brain.

## REFERENCES AND NOTES

1. S. Ramon y Cajal, *Histologie du Système Nerveux de l'Homme et des Vertébrés* (Maloine, Paris, 1911); G. M. Shepherd, in *Handbook of Physiology, Section 1: The Nervous System*, E. R. Kandel, Ed. (American Physiological Society: Bethesda, MD, 1977), vol. 1, part 2, pp. 945-968; J. W. Scott and T. A. Harrison, in *Neurobiology of Taste and Smell*, T. E. Finger and W. L. Silver, Eds. (Wiley, New York, 1987), pp. 151-178; K. Mori, *Prog. Neurobiol.* **29**, 275 (1987).
2. W. Rall, G. M. Shepherd, T. S. Reese, M. W. Brightman, *Exp. Neurol.* **14**, 44 (1966); W. Rall and G. M. Shepherd, *J. Neurophysiol.* **31**, 884 (1968); C. E. Jahr and R. A. Nicoll, *J. Physiol. (London)* **326**, 213 (1982).
3. G. M. Shepherd and C. A. Greer, in *The Synaptic Organization of the Brain*, G. M. Shepherd, Ed. (Oxford Univ. Press, New York, ed. 3, 1990), pp. 133-169.
4. The experiments were performed on  $400$ - $\mu$ m-thick slices horizontally cut from the olfactory bulbs of Sprague-Dawley rats (18 to 28 days old). Slices were prepared following previously published procedures (5, 6) and were perfused with an oxygenated Ringer solution containing  $124$  mM NaCl,  $3$  mM KCl,  $1.3$  mM  $MgSO_4$ ,  $2$  mM  $CaCl_2$ ,  $1.25$  mM  $NaH_2PO_4$ ,  $26$  mM  $NaHCO_3$ , and  $10$  mM glucose (pH 7.4). Most experiments were carried out at room temperature; several experiments performed at  $37^\circ$ C showed similar results. For viewing slices, an Olympus BX50WI infrared DIC microscope was equipped with a  $40\times$  water-immersion objective and a Hamamatsu C2400-07ER camera. For dendritic recordings, a high-magnification image was obtained by switching to a light path with a  $3.3\times$  photo-eyepiece and a Dage-MTI CCD-72 camera. The recording pipettes were made from thick-walled glass capillaries ( $1.2$  mm outer diameter,  $0.69$  mm inner diameter) and had a resistance of  $10$  to  $12$  megohms when filled with a solution composed of  $110$  mM K-gluconate,  $2$  mM  $MgSO_4$ ,  $10$  mM HEPES, and  $2$  mM  $K_2$ -adenosine triphosphate (adjusted to pH 7.2 to 7.3 and osmolality of  $290$  to  $300$  mosM with KOH and sucrose, respectively). The measured liquid junction potential of the pipette solution was  $-15$  mV with respect to the Ringer solution, and this offset was corrected in all recordings. The low chloride concentration in the pipette solution gave a relatively negative inhibitory equilibrium potential, which helped to maintain strong inhibition of mitral cells by the granule cell interneuronal population as seen in vivo (see text). Experiments with  $8$  mM  $Cl^-$  in the pipette have given similar results. The criteria for data analysis were a resting membrane potential greater than  $-50$  mV and an overshooting somatic action potential. In some experiments,  $0.1\%$  biocytin and  $0.1\%$  lucifer yellow potassium salt were included in the pipette solution to analyze the morphology of recorded mitral cells. Recordings were made in bridge mode using an Axoclamp-2A amplifier (bandpass: DC- $30$  kHz). In order to achieve a fast sampling rate for two channels of membrane potential and two channels of membrane current, we employed two computer systems synchronized by an external trigger. Membrane potentials were digitized at  $20$  kHz with an Instrutech ITC-16 interface and a PowerMac computer. Membrane currents were recorded at  $2.5$  kHz with an Axon TL-1 interface and an IBM-compatible 486 computer. The positions of recording and stimulating electrodes were photographed with a Scion LG-3 frame grabber, and the distance between the somatic and dendritic recording sites was measured on the computer. To stimulate the olfactory nerve, a concentric bipolar electrode (tip diameter of  $25$   $\mu$ m) was placed in the olfactory nerve layer just above the glomerulus to which the recorded mitral cell projected its primary dendrite. Another stimulating electrode was located laterally in the deep EPL to elicit inhibitory synaptic input to the secondary dendrites of the recorded mitral cell. This electrode was generally  $300$  to  $800$   $\mu$ m from the recorded mitral cell primary dendrite. The stimulating electrodes were connected to two electronic isolators, and constant current stimuli of variable strength ( $10$   $\mu$ A to  $2$  mA) were delivered.
5. W. T. Nickell, M. T. Shipley, M. M. Behbehani, *Brain Res. Bull.* **39**, 57 (1996); M. Ennis, L. A. Zimmer, M. T. Shipley, *Neuroreport* **7**, 989 (1996); G. J. Stuart, H.-U. Dodt, B. Sakmann, *Pflügers Arch. Eur. J. Physiol.* **423**, 511 (1993).
6. W. R. Chen and G. M. Shepherd, *Brain Res.* **745**, 189 (1997).
7. D. B. Jaffe et al., *Nature* **357**, 244 (1992); G. J. Stuart and B. Sakmann, *ibid.* **367**, 69 (1994); N. Spruston, Y. Schiller, G. Stuart, B. Sakmann, *Science* **268**, 297 (1995); K. Svoboda, W. Denk, D. Kleinfeld, D. W. Tank, *Nature* **385**, 161 (1997); J. C. Magee and D. A. Johnston, *Science* **275**, 209 (1997).
8. W. R. Chen, J. Midtgaard, G. M. Shepherd, data not shown.
9. J. Levetau and P. MacLeod, *Science* **175**, 170 (1965); J. S. Kauer, *J. Physiol. (London)* **243**, 695 (1975); D. P.

- Wellis and J. W. Scott, *Chem. Senses* **12**, 707 (1987); K. A. Hamilton and J. S. Kauer, *Brain Res.* **338**, 181 (1989).
10. M. Häusser, G. Stuart, C. Racca, B. Sakmann, *Neuron* **15**, 637 (1995).
  11. W. A. Spencer and E. R. Kandel, *J. Neurophysiol.* **24**, 272 (1961).
  12. K. Mori, M. C. Nowycky, G. M. Shepherd, *J. Neurosci.* **2**, 497 (1982); K. Mori and S. F. Takagi, *Brain Res.* **100**, 685 (1975).
  13. H.-T. Chang, *Cold Spring Harbor Symp. Quant. Biol.* **17**, 189 (1952); B. G. Cragg and L. H. Hamlyn, *J. Physiol. (London)* **129**, 608 (1955); L. S. Benardo, L. M. Masukawa, D. A. Prince, *J. Neurosci.* **2**, 1614 (1982); J. R. Huguenard, O. P. Hamill, D. A. Prince, *Proc. Natl. Acad. Sci. U.S.A.* **86**, 2473 (1989); O. Herreras, *J. Neurophysiol.* **64**, 1429 (1990); R. W. Turner, D. E. R. Meyers, T. L. Richardson, J. L. Barker, *J. Neurosci.* **11**, 2270 (1991).
  14. W. G. Regehr and C. M. Armstrong, *Curr. Biol.* **4**, 436 (1994).
  15. G. Stuart, N. Spruston, B. Sakmann, M. Häusser, *Trends Neurosci.* **20**, 125 (1997).
  16. J. DeFelipe and I. Farinas, *Prog. Neurobiol.* **39**, 563 (1992).
  17. Z. F. Mainen, J. Joerges, J. R. Huguenard, T. J. Sejnowski, *Neuron* **15**, 1427 (1995).
  18. J. C. Callaway, N. Lasser-Ross, W. N. Ross, *J. Neurosci.* **15**, 2777 (1995); H. Tsubokawa and W. N. Ross, *J. Neurophysiol.* **76**, 2896 (1996).
  19. This work was supported by grants from the National Institute on Deafness and Other Communication Disorders (NIDCD) and by the National Institute of Mental Health, NASA, and NIDCD under the Human Brain Project (G.M.S.), and by grants from the Carlsberg Foundation, the Danish Medical Research Council, the Faculty of Health Sciences (Copenhagen University), and the Danish Medical Association's Research Fund (J.M.).

3 July 1997; accepted 4 September 1997

## Mediation of Classical Conditioning in *Aplysia californica* by Long-Term Potentiation of Sensorimotor Synapses

Geoffrey G. Murphy and David L. Glanzman\*

Long-term potentiation (LTP) is considered an important neuronal mechanism of learning and memory. Currently, however, there is no direct experimental link between LTP of an identified synapse and learning. A cellular analog of classical conditioning in *Aplysia* was used to determine whether this form of invertebrate learning involves *N*-methyl-D-aspartate (NMDA)-type LTP. The NMDA receptor-antagonist DL-2-amino-5-phosphonovalerate significantly disrupted synaptic enhancement after associative training but did not disrupt synaptic enhancement after nonassociative training. Thus, classical conditioning in *Aplysia* appears to be mediated, in part, by LTP due to activation of NMDA-related receptors.

LTP of *Aplysia* sensorimotor synapses, like LTP of synapses in the CA1 region of the mammalian hippocampus (1), requires strong postsynaptic depolarization and postsynaptic influx of  $\text{Ca}^{2+}$  (2, 3). Furthermore, induction of LTP of *Aplysia* sensorimotor synapses also resembles LTP of CA1 synapses (4) in its requirement for activation of NMDA-type receptors (5) because it can be inhibited by the vertebrate NMDA receptor-antagonist DL-2-amino-5-phosphonovalerate (APV) (3). The finding (3) that LTP of the sensorimotor synapses can be induced in Hebbian (6) fashion raises the possibility that LTP might mediate classical conditioning of the siphon-withdrawal reflex of *Aplysia* (7). Tail shock, the unconditioned stimulus (US) for this form of associative learn-

ing, strongly depolarizes, and typically fires, the siphon motor neurons (8). Thus, paired presentation of the conditioned stimulus (CS)—weak tactile stimulation of the animal's siphon or mantle—and the US during conditioning should produce a pattern of neural activity within the nervous system of *Aplysia* like that used to induce Hebbian LTP of in vitro sensorimotor synapses (3): brief firing of the sensory neurons paired with strong depolarization of the motor neurons (9). Support for the idea that classical conditioning in *Aplysia* might involve LTP of sensorimotor synapses comes from the finding that infusing the postsynaptic motor neuron with the  $\text{Ca}^{2+}$  chelator 1,2-bis(2-aminophenoxy) ethane-*N,N,N',N'*-tetraacetic acid (BAPTA) blocks a cellular analog of classical conditioning (10).

In this study, we tested the hypothesis (3, 11) that classical conditioning of the siphon-withdrawal reflex of *Aplysia* is mediated, in part, by NMDA receptor-type LTP. Accordingly, we examined whether the cellular analog of classical conditioning of this reflex (12) was disrupted when training was

carried out in the presence of APV. We assessed the strength of the synapse between a siphon sensory neuron and a siphon motor neuron in the abdominal ganglion before, during, and after conditioning-related training (13). For this cellular analog of classical conditioning, the CS was brief intracellular stimulation of the sensory neuron and the US was extracellular stimulation of the tail (P9) nerves (Fig. 1A). Some preparations received the paired CS-US stimuli in artificial seawater (ASW) containing APV (100  $\mu\text{M}$ ) (14). We also included two groups of untrained preparations that received the test stimuli but not the paired stimuli. One untrained group (Test alone) received the test stimuli in normal ASW; the other untrained group (Test alone-APV) received the test stimuli in ASW containing APV. Furthermore, we carried out additional control experiments in which the CS and US were delivered in unpaired fashion in the presence and absence of APV (see below).

The monosynaptic sensorimotor excitatory postsynaptic potentials (EPSPs) in preparations that received only the test stimuli in ASW exhibited the homosynaptic depression characteristic of *Aplysia* sensorimotor synapses (Fig. 1, B and C) (15–17). The presence of APV did not significantly affect this homosynaptic depression, as indicated by the Test alone-APV data (17, 18). The monosynaptic EPSPs in preparations that received paired presentations of the CS and US in normal ASW (CS<sup>+</sup> group) were significantly enhanced on both the 15- and 60-min posttests compared with the pretest EPSPs as well as with the EPSPs of Test alone preparations on the posttests (18). The presence of APV during training significantly disrupted the synaptic enhancement produced by paired stimulation. However, APV did not completely eliminate this synaptic enhancement; the mean amplitude of the CS<sup>+</sup>-APV EPSPs was significantly greater than that of the Test alone-APV EPSPs on the 15-min posttest (Fig. 1, B and C; CS<sup>+</sup>-APV data). The paired stimulation also produced strong enhancement of the amplitude of the potentially polysynaptic sensorimotor EPSPs evoked on the test trials during training. This enhancement was reduced in the presence of APV, albeit not significantly so (19).

A possible explanation for the reduced enhancement of the monosynaptic sensorimotor connection after training in APV is that the drug might have disrupted the activity, or efficacy, of endogenous facilitatory interneurons, which are activated in *Aplysia* by US-related stimuli (8, 20, 21). To test this possibility, we carried out experiments similar to those described above but with a specifically unpaired training protocol. Such a protocol induces presynap-

G. G. Murphy, Interdepartmental Graduate Program in Neuroscience, School of Medicine, University of California, Los Angeles, CA 90095, USA.

D. L. Glanzman, Department of Physiological Science and Brain Research Institute, University of California, 2859 Slichter Hall, Los Angeles, CA 90095-1568, USA.

\*To whom correspondence should be addressed. E-mail: dgglanzman@physci.ucla.edu